JACS
JOURNAL OF THE AMERICAN CHEMICAL SOCIETY

COMMUNICATION

pubs.acs.org/JACS

Translational Diffusion of Macromolecular Assemblies Measured Using Transverse-Relaxation-Optimized Pulsed Field Gradient NMR

Reto Horst,[†] Arthur L. Horwich,[†,§] and Kurt Wüthrich*[,†,‡]

[†]Department of Molecular Biology and [‡]The Skaggs Institute for Chemical Biology, The Scripps Research Institute, 10550 North Torrey Pines Road, La Jolla, California 92037, United States

[§]Howard Hughes Medical Institute and Institute of Genetics, Yale University School of Medicine, New Haven, Connecticut 06510, United States

Supporting Information

ABSTRACT: In structural biology, pulsed field gradient (PFG) NMR spectroscopy for the characterization of size and hydrodynamic parameters of macromolecular solutes has the advantage over other techniques that the measurements can be recorded with identical solution conditions as used for NMR structure determination or for crystallization trials. This paper describes two transverse-relaxation-optimized (TRO) ^{15}N-filtered PFG stimulated-echo (STE) experiments for studies of macromolecular translational diffusion in solution, ^{1}H-TRO-STE and ^{15}N-TRO-STE, which include CRINEPT and TROSY elements. Measurements with mixed micelles of the *Escherichia coli* outer membrane protein X (OmpX) and the detergent Fos-10 were used for a systematic comparison of ^{1}H-TRO-STE and ^{15}N-TRO-STE with conventional ^{15}N-filtered STE experimental schemes. The results provide an extended platform for evaluating the NMR experiments available for diffusion measurements in structural biology projects involving molecular particles with different size ranges. An initial application of the ^{15}N-TRO-STE experiment with very long diffusion delays showed that the tedradecamer structure of the 800 kDa *Thermus thermophilus* chaperonin GroEL is preserved in aqueous solution over the temperature range 25−60 °C.

This communication evaluates and applies transverse relaxation optimization (TRO) in NMR experiments that are used to measure translational diffusion of macromolecular solutes in liquids. Renewed interest in hydrodynamic measurements has been generated by the increased focus of structural biology on supramolecular structures, which requires analytical tools for the characterization of entities consisting of two or multiple noncovalently linked molecules. Among the methods used, which also include ultracentrifugation, quasi-elastic light scattering, small-angle X-ray scattering, and small-angle neutron scattering, pulsed field gradient (PFG) NMR spectroscopy has the advantage that the measurements can be carried out under conditions of protein and detergent concentrations, ionic strength, and temperature that are closely similar to those used for NMR structure determination and crystallization trials. In line with the aforementioned interest in hydrodynamic studies of supramolecular structures, prominent applications of PFG-NMR diffusion measurements include monitoring of protein association,[1−4] characterization of protein−ligand interactions,[5−7] and determination of the size and shape of detergent micelles and membrane protein−detergent mixed micelles.[8−11]

NMR diffusion measurements initially used the spin-echo (SE) experiment.[12] Subsequently the stimulated-echo (STE) experiment, which enables storage of the magnetization along the z axis during waiting periods when it is not being dephased or rephased by magnetic field gradients,[13] has been widely used for studies of macromolecular systems with slow longitudinal relaxation and fast transverse relaxation (i.e., with $T_1 \gg T_2$, where T_1 and T_2 are the longitudinal and transverse nuclear spin relaxation times, respectively). More recently, heteronuclear filters were incorporated into STE pulse sequences to distinguish between signals arising from stable-isotope-labeled and -unlabeled components in the solutions studied,[14] and the X-STE experiment[15,16] was designed to extend the size limit for measurements of diffusion coefficients of isotope-labeled molecules beyond the STE limit of ∼50 kDa. This was achieved by storing the magnetization during the diffusion delay on either ^{15}N or ^{13}C spins, both of which have lower relaxation rates than ^{1}H spins in the same protein. Although the diffusion interval in X-STE could thus be increased ∼10-fold relative to STE,[15] transverse relaxation during the INEPT ^{15}N,^{1}H magnetization transfer steps became a limiting factor when working with large molecular sizes. To extend the size range further, we have now replaced the INEPT coherence transfers in ^{15}N-filtered PFG-STE experiments by CRINEPT.[17] Studies of mixed micelles of the outer membrane protein X from *Escherichia coli* (OmpX) and the detergent Fos-10 with the experiments ^{1}H-TRO-STE and ^{15}N-TRO-STE were used to compare the performance of corresponding experiments with and without TRO. The ^{15}N-TRO-STE experiment was then applied for studies of the hydrodynamic properties of the 800 kDa tetradecameric chaperonin protein GroEL from *Thermus thermophilus*[18,19] under variable solution conditions.

The ^{1}H-TRO-STE experimental scheme (Figure 1A) is based on a heteronuclear-filtered PFG-STE experiment (Figure 1C in Tillet et al.[6]) in which the magnetization is stored in the bilinear H_zN_z state during the delay T. In ^{1}H-TRO-STE the delay τ_H is adjusted for optimal CRINEPT transfer[17] rather than being set to $|2J_{HN}|^{-1} = 5.4$ ms.[6] To avoid radiation damping during the diffusion delay and prevent saturation of the labile protein protons, water-selective soft pulses are applied to keep the bulk water magnetization along the z axis during the entire course of the experiment, and no ^{15}N-decoupling is applied during acquisition in order to benefit from the ^{15}N−^{1}H

Received: July 20, 2011
Published: September 16, 2011

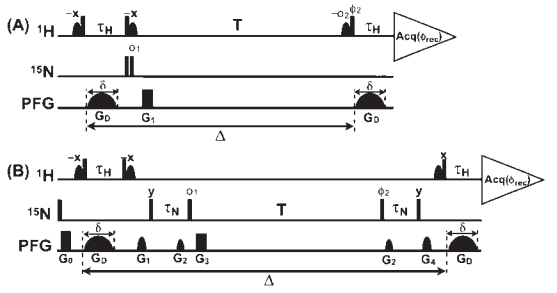

Figure 1. TRO-STE (*t*ransverse-*r*elaxation-*o*ptimized ^{15}N-filtered PFG *st*imulated-*e*cho) pulse schemes for measuring translational self-diffusion coefficients D_t, of macromolecules in solution. Vertical bars on the lines marked ^{1}H and ^{15}N indicate nonselective 90° pulses, and sine-bell shapes on the ^{1}H line indicate water-selective 90° pulses. The line marked PFG indicates the durations and shapes of pulsed magnetic field gradients applied along the *z* axis. The gradients G_D, which encode the variable diffusion delay (Δ), have adjustable amplitudes and a fixed duration (δ) of 4.5 ms. The "crusher gradients" G_0 to G_4 are used to dephase unwanted magnetization. The CRINEPT transfer delay τ_H can be optimized using CRINEPT buildup measurements,[17] and τ_N can be adjusted for high sensitivity using a ^{15}N-TRO-STE experiment with constant G_D amplitude. For both delays, the typical lengths thus found are between 3.0 and 5.4 ms. (A) ^{1}H-TRO-STE. For the applications in this paper, the duration and strength of the rectangular gradient G_1 were 500 μs and 31 G/cm. Phase cycling: $\phi_1 = x, -x, x, -x$; $\phi_2 = x, x, y, y$; $\phi_{rec} = x, -x, -x, x$. (B) ^{15}N-TRO-STE. Duration, strength, and shape of the gradients G_0 to G_4: G_0, 1 ms, 27 G/cm, rectangular; G_1, 0.5 ms, 23 G/cm, sine-bell; G_2, 0.3 ms, 13 G/cm, sine-bell; G_3, 0.5 ms, 31 G/cm, rectangular; G_4, 0.5 ms, 21 G/cm, sine-bell. Phase cycling: $\phi_1 = y, -y, y, -y$; $\phi_2 = y, y, -y, -y$; $\phi_{rec} = x, -x, -x, x$.

TROSY effect.[19] The ^{15}N-TRO-STE scheme (Figure 1B) has in common with the X-STE experiment of Ferrage et al.[15] that losses due to longitudinal relaxation are reduced by keeping the magnetization in the N_z state during the delay T. Furthermore, to achieve efficient TRO, we introduced an ^{1}H-to-^{15}N magnetization transfer element consisting of two consecutive CRINEPT steps (τ_H and τ_N) and added ^{15}N−^{1}H TROSY by eliminating ^{15}N decoupling during acquisition. In the practice of PFG-STE experiments, one measures the ratio of a signal *S*, which is recorded with variable amplitudes of the gradient pulse G_D and therefore is attenuated by diffusion, and a reference signal S_0, which is recorded with very weak G_D amplitudes:

$$S/S_0 = \exp[-q^2 D_t(\Delta - \delta/3)] \quad (1)$$

In eq 1, $q = \gamma_H s G_D \delta$ is the area of the gradient pulse G_D, where γ_H is the proton gyromagnetic ratio and *s* represents the shape of the diffusion gradient with peak amplitude G_D and duration δ, D_t is the translational diffusion constant, and Δ is the diffusion delay (Figure 1). Both S_0 and *S* are dampened by longitudinal ^{1}H and ^{15}N relaxation during the delay T, affected by transverse ^{1}H and ^{15}N relaxation during the transfer periods τ_H and τ_N, and modulated by scalar couplings. The resulting signal attenuation can be described by the factors $f_{H\text{-TRO-STE}}$ and $f_{N\text{-TRO-STE}}$:

$$f_{H\text{-TRO-STE}} = \Lambda_H e^{-\Gamma_{H_zN_z,H_zN_z}T - 2\bar{\Gamma}_H\tau_H} \quad (2)$$

$$f_{N\text{-TRO-STE}} = 0.5\Lambda(\Lambda_N e^{-\Gamma_{N_z,N_z}T} + K_N e^{-\Gamma_{H_zN_z,H_zN_z}T}) e^{-2\bar{\Gamma}_H\tau_H - 2\bar{\Gamma}_N\tau_N} \quad (3)$$

in which Γ_{N_z,N_z} and $\Gamma_{H_zN_z,H_zN_z}$ are the longitudinal relaxation rate constants for the N_z and the H_zN_z states, respectively, and $\bar{\Gamma}_H$ and $\bar{\Gamma}_N$ are average transverse autorelaxation rate constants of in-phase and antiphase ^{15}N and ^{1}H coherences:[20,21]

$$\bar{\Gamma}_H = (\Gamma_{H^+,H^+} + \Gamma_{H^+N_z,H^+N_z})/2 \quad (4)$$

$$\bar{\Gamma}_N = (\Gamma_{N^+,N^+} + \Gamma_{H_zN^+,H_zN^+})/2 \quad (5)$$

For ^{15}N-TRO-STE, the signal attenuation caused by diffusion between the two gradients G_2 (length, 0.3 ms; gradient strength, 13 G/cm) was estimated to be <1 ‰ even for long diffusion delays (Δ = 1 s) and fast diffusion ($D_t = 2 \times 10^{-10}$ m^2/s), and it was therefore not considered in eq 3.

The coefficients Λ_H, Λ_N, and K_N are given by eqs 6−8, in which $\Gamma^{DD/CSA}_{H^+,H^+N_z}$ and $\Gamma^{DD/CSA}_{N^+,H_zN^+}$ are the transverse ^{1}H and ^{15}N cross-correlated relaxation rate constants:

$$\Lambda_H = \sinh^2(\Gamma^{DD/CSA}_{H^+,H^+N_z}\tau_H) + \sin^2(\pi J_{HN}\tau_H) \quad (6)$$

$$\Lambda_N = \sinh^2(\Gamma^{DD/CSA}_{N^+,H_zN^+}\tau_N) + \sin^2(\pi J_{HN}\tau_N) \quad (7)$$

$$K_N = \cosh^2(\Gamma^{DD/CSA}_{N^+,H_zN^+}\tau_N) - \sin^2(\pi J_{HN}\tau_N) \quad (8)$$

Equations 6−8 describe linear combinations of polarization transfers via scalar coupling (sine function) and CRIPT (hyperbolic sine and cosine functions). For short rotational correlation times τ_c, the cross-correlated relaxation rate constants $\Gamma^{DD/CSA}_{H^+,H^+N_z}$ and $\Gamma^{DD/CSA}_{N^+,H_zN^+}$ are negligibly small, and only the INEPT pathway, given by the second term in eqs 6−8, contributes significantly to the CRINEPT transfer; on the other hand, for τ_c values >100 ns, $\Gamma^{DD/CSA}_{H^+,H^+N_z}$ and $\Gamma^{DD/CSA}_{N^+,H_zN^+}$ become large, and CRIPT is the dominant polarization transfer mechanism in the CRINEPT element.[17] In the absence of spin relaxation, the signal intensity in the ^{15}N-TRO-STE experiment would be reduced by a factor of 2 relative to other STE-type experiments (see eqs 2 and 3). Nonetheless, model calculations of the relative sensitivities of the ^{15}N-TRO-STE, ^{1}H-TRO-STE, and X-STE experiments for translational diffusion measurements predict that ^{15}N-TRO-STE is a promising approach for studies of large supramolecular structures with rapid transverse spin relaxation [Figure S1 in the Supporting Information (SI)].

For an experimental validation of the predictions in Figure S1, we recorded ^{15}N-TRO-STE, ^{1}H-TRO-STE, and X-STE experiments on [U-^{15}N,U∼80%-^{2}H]-labeled OmpX reconstituted in mixed micelles with Fos-10 using Δ values (Figure 1) ranging from 100 to 300 ms. At a sample temperature of 4 °C, the effective rotational correlation time τ_c for OmpX/Fos-10 micelles was 52 ns, as determined using the TRACT experiment.[22] For this system, ^{15}N-TRO-STE is ∼1.5-fold more sensitive than X-STE (Figure 2B,C), which reflects the higher efficiency of the CRINEPT transfers[17] used in ^{15}N-TRO-STE relative to the INEPT transfers in the X-STE experiment. This gain is close to the 1.3-fold increase in sensitivity of ^{15}N-TRO-STE over the X-STE experiment predicted for uniformly 80% ^{2}H-labeled antiparallel β-sheets in particles with the size of OmpX/Fos-10 micelles (Figure S1A). For a diffusion delay of 100 ms, the ^{1}H-TRO-STE experiment was ∼2-fold more sensitive than ^{15}N-TRO-STE, but its signal intensity fell off rapidly for longer Δ (Figure 2A). The small loss of ^{15}N-TRO-STE signal intensity between Δ values of 100 and 300 ms (Figure 2B) probably arises primarily because the K_N magnetization transfer pathway (eq 3) becomes less efficient for long diffusion delays as a result of longitudinal proton relaxation of the H_zN_z state.

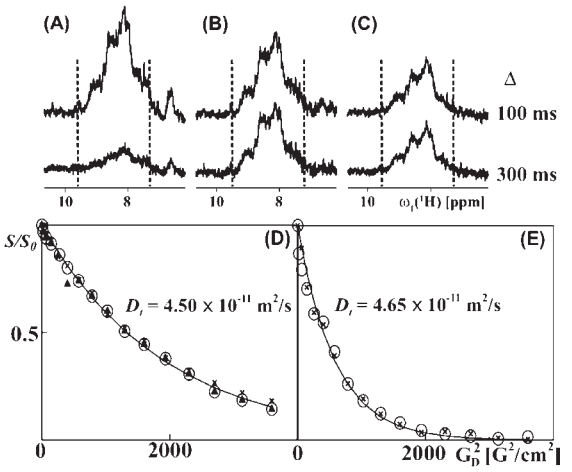

Figure 2. Experimental comparison of the ^{1}H-TRO-STE, ^{15}N-TRO-STE, and X-STE pulse schemes for translational diffusion measurements based on data collected with [U-^{15}N,U∼80%-^{2}H]-labeled OmpX in mixed micelles with the unlabeled detergent Fos-10 at 4 °C. (A−C) 1D ^{15}N-filtered ^{1}H NMR spectra measured using ^{1}H-TRO-STE, ^{15}N-TRO-STE, and X-STE, respectively, with gradient strengths G_D of 3 G/cm and diffusion delays Δ (see Figure 1) of 100 and 300 ms. The signal intensity between the broken vertical lines was evaluated in order to obtain the values for S_0 and S that were used in eq 1 to determine the diffusion constants indicated in (D) and (E). (D, E) NMR data used to determine the diffusion constant acquired with (D) Δ = 100 ms and (E) Δ = 300 ms. The relative signal intensities are plotted vs the square of the gradient strength. In (D), ▲, ×, and ○ symbols represent the data obtained with ^{1}H-TRO-STE, X-STE, and ^{15}N-TRO-STE, respectively. In (E), only the X-STE and ^{15}N-TRO-STE data are shown. Translational diffusion constants D_t as calculated from the ^{15}N-TRO-STE data using a single-exponential fit are shown. For the TRO-STE experiments, the encoding gradients δ (Figure 1) had a length of 4.5 ms. For the X-STE experiment, bipolar gradients with a length of 2.25 ms were used.[15] Each 1D spectrum was obtained by accumulating 128 transients in 5 min.

For measurements of diffusion constants, the amplitude of the gradients G_D (Figure 1) was incremented linearly in 16 steps. The resulting decay of the signal intensity as a function of G_D^2 is single-exponential, as predicted by eq 1, yielding values of (4.50−4.65) × 10^{-11} m^2/s for the diffusion coefficient of OmpX/Fos-10 micelles (Figure 2D,E). Overall, the model calculations (Figure S1) and the experiments with OmpX/Fos-10 mixed micelles (Figure 2) yielded three key results. First, the ^{1}H-TRO-STE scheme provides high sensitivity for work with small molecular particles that can be studied with Δ values (Figure 1A) up to ∼100 ms. ^{1}H-TRO-STE may therefore become an attractive alternative to other experiments[12−16] available for studies of molecular sizes corresponding to τ_c values up to ∼40 ns. Second, for measurements with diffusion delays Δ longer than 100 ms, as needed for studies of large molecular sizes, the ^{15}N-TRO-STE scheme yields the best sensitivity. Third, identical translational diffusion coefficients for OmpX/Fos-10 mixed micelles were obtained with either of the three experimental schemes used in Figure 2A−C with Δ = 100 ms, and a closely similar value was obtained with Δ = 300 ms [because of the low sensitivity (Figure 2A), the ^{1}H-TRO-STE data obtained with Δ = 300 ms were not included in Figure 2E]. For each size range, one may thus select the experimental scheme that yields the best sensitivity without running risks that the diffusion measurements might be biased by the selection of the particular experiment.

For an initial assessment of the uniformly [^{2}H,^{15}N]-labeled chaperonin *T. thermophilus* GroEL, we measured ^{15}N−^{1}H NMR correlation spectra. Key observations resulted from the temperature dependence of the 2D [^{15}N,^{1}H]-TROSY spectrum on the one hand and the 2D [^{15}N,^{1}H]-CRIPT-TROSY spectrum on the other (Figure 3). The small dispersion of the resonances along the ω_2(^{1}H) axis in the 2D [^{15}N,^{1}H]-TROSY spectrum at 25 °C (Figure 3A) indicates that the observed signals are from flexibly disordered polypeptide segments devoid of regular secondary structure.[23] This is in line with previous studies,[24,25] which had shown that transverse relaxation is too fast to allow observation of NMR signals from structured polypeptide segments within particles having masses of several hundred kilodaltons in 2D [^{15}N,^{1}H]-TROSY spectra recorded at room temperature. The spectrum of Figure 3A is strikingly different from the widely dispersed 2D [^{15}N,^{1}H] correlation map with more than 300 resolved cross-peaks (Figure 3B) that was obtained from the 2D [^{15}N,^{1}H]-TROSY measurement at 60 °C and is typical for a folded globular protein. In contrast, the 2D [^{15}N,^{1}H]-CRIPT-TROSY spectra recorded at 25 and 60 °C have similar overall features (Figure 3C,D) and also show dispersion of the ^{1}H chemical shifts comparable to that in the [^{15}N,^{1}H]-TROSY spectrum at 60 °C (Figure 3B).

For a more detailed interpretation of the data in Figure 3, in particular in view of the extensive differences between the [^{15}N,^{1}H]-TROSY spectra at 25 and 60 °C (Figure 3A,B), it was of interest to characterize the oligomeric state of *T. thermophilus* GroEL at the different temperatures used. We therefore performed ^{15}N-TRO-STE experiments to determine the translational diffusion coefficient of *T. thermophilus* GroEL ($D_{t,EL}$) at 25 and 60 °C (Figure 3E). We further determined the diffusion coefficient of the internal standard DSS ($D_{t,DSS}$) at the same temperatures and calculated the relative diffusivity of *T. thermophilus* GroEL (d_{EL}) using eq S1 in the SI. It has been shown previously that convection in the sample can lead to an overestimation of D_t in PFG-STE exeriments.[26] Jerschow and Müller[27] have developed elegant NMR experiments to eliminate these convection artifacts, but these methods are difficult to implement into X-STE-type experiments. We therefore chose the alternative of working with samples having restricted volumes.[15] To assess the influence of convection on the measured D_t values at 60 °C, we performed PFG-STE experiments on HDO at various temperatures and diffusion delays (Figure S2) and found that by using the experimental setup described in Methods in the SI, D_t measurements at 60 °C were not measurably affected by convection.

The value of 3.8 × 10^{-11} m^2/s for $D_{t,EL}$ at 25 °C (Table S1) is much smaller than the D_t value expected for a 58 kDa *T. thermophilus* GroEL monomer, and it is characteristic of a large particle in the molecular size range of tetradecameric *T. thermophilus* GroEL.[28] The value of $D_{t,DSS}$ is 2.4 times larger at 60 °C than at 25 °C (Table S1), which is in satisfactory agreement with the increase by a factor 2.1 that is predicted on the basis of the temperature dependence of the viscosity (η) for H_2O.[29] Finally, the relative diffusivity d_{EL} for *T. thermophilus* GroEL, which is independent of the solvent viscosity and the temperature, has very similar values at 25 and 60 °C (Table S1). The combined data on GroEL and DSS then show that the value of 10.1 × 10^{-11} m^2/s for $D_{t,EL}$ at 60 °C can be rationalized by the decrease in η with increasing temperature and that the tetradecameric state of *T. thermophilus* GroEL is highly populated also at 60 °C. The improved quality of the 2D [^{15}N,^{1}H]-TROSY spectrum of *T. thermophilus* GroEL at 60 °C in comparison with the corresponding spectrum at 25 °C (Figure 3A,B) is therefore due to the shorter effective τ_c value resulting from the reduced solvent viscosity at

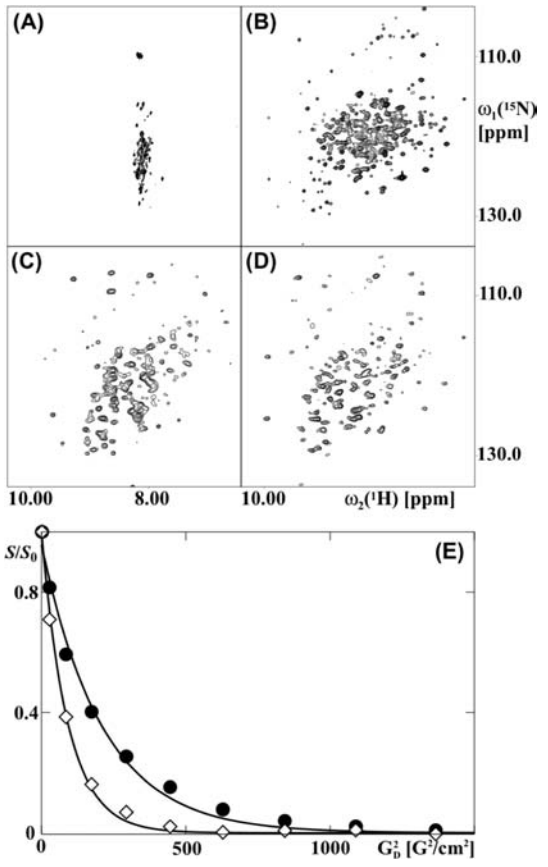

Figure 3. NMR spectra and diffusion measurements of the uniformly [^{15}N,^{2}H]-labeled 800 kDa protein GroEL from *T. thermophilus*. (A, B) 2D [^{15}N,^{1}H]-TROSY spectra acquired at (A) 25 and (B) 60 °C. (C, D) 2D [^{15}N,^{1}H]-CRIPT-TROSY spectra acquired at (C) 25 and (D) 60 °C with CRIPT transfer delays of 1.0 and 2.0 ms, respectively. (E) NMR data used to determine the diffusion constant, D_t, with ^{15}N-TRO-STE experiments at 25 °C (●) and 60 °C (◇). The spectra were recorded with δ = 4.5 ms and Δ = 800 ms (see Figure 1). S and S_0 were evaluated as sums of the signal intensities in the ^{1}H chemical shift range 8.7−9.6 ppm. The resulting D_t values were determined by fitting the data to eq 1 (see Table S1). The parameter settings used to collect and process the data are described in Methods in the SI.

60 °C and not to dissociation of the tetradecameric functional state of the chaperonin.

In conclusion, the ^{1}H-TRO-STE and ^{15}N-TRO-STE experiments introduced here enable improved measurements of the translational diffusion coefficients for ^{15}N-labeled polypeptides in large complexes. In particular, the fully transverse-relaxation-optimized ^{15}N-TRO-STE experiment allows the determination of small diffusion coefficients of polypeptide chains in supramolecular structures with masses of several hundred kilodaltons.

■ ASSOCIATED CONTENT

Supporting Information. Bruker AVANCE pulse programs for H-TRO-STE (listing S1) and N-TRO-STE (listing S2), materials and methods, and additional data. This material is available free of charge via the Internet at http://pubs.acs.org.

■ AUTHOR INFORMATION

Corresponding Author
wuthrich@scripps.edu

■ ACKNOWLEDGMENT

We thank Drs. George W. Farr and Navneet K. Tyagi for help with the preparation of *T. thermophilus* GroEL. This work was supported by the Joint Center for Innovative Membrane Protein Technologies (JCIMPT; NIH Roadmap Initiative Grant P50GM073197 for technology development). K.W. is the Cecil H. and Ida M. Green Professor of Structural Biology at The Scripps Research Institute.

■ REFERENCES

(1) Altieri, A. S.; Hinton, D. P.; Byrd, R. A. *J. Am. Chem. Soc.* **1995**, *117*, 7566.
(2) Dingley, A.; Mackay, J.; Chapman, B.; Morris, M.; Kuchel, P.; Hambly, B.; King, G. *J. Biomol. NMR* **1995**, *6*, 321.
(3) Ilyina, E.; Roongta, V.; Pan, H.; Woodward, C.; Mayo, K. *Biochemistry* **1997**, *36*, 3383.
(4) Krishnan, V. *J. Magn. Reson.* **1997**, *124*, 468.
(5) Hajduk, P. J.; Olejniczak, E. T.; Fesik, S. W. *J. Am. Chem. Soc.* **1997**, *119*, 12257.
(6) Tillett, M.; Horsfield, M.; Lian, L.-Y.; Norwood, T. *J. Biomol. NMR* **1999**, *13*, 223.
(7) Hodge, P.; Monvisade, P.; Morris, G. A.; Preece, I. *Chem. Commun.* **2001**, 239.
(8) Vinogradova, O.; Sonnichsen, F.; Sanders, C. *J Biomol NMR* **1998**, *11*, 381.
(9) Chou, J. J.; Baber, J. L.; Bax, A. *J. Biomol. NMR* **2004**, *29*, 299.
(10) Krueger-Koplin, R.; Sorgen, P.; Krueger-Koplin, S.; Rivera-Torres, I. O.; Cahill, S.; Hicks, D.; Grinius, L.; Krulwich, T.; Girvin, M. *J. Biomol. NMR* **2004**, *28*, 43.
(11) Stanczak, P.; Horst, R.; Serrano, P.; Wüthrich, K. *J. Am. Chem. Soc.* **2009**, *131*, 18450.
(12) Stejskal, E. O.; Tanner, J. E. *J. Chem. Phys.* **1965**, *42*, 288.
(13) Tanner, J. E. *J. Chem. Phys.* **1970**, *52*, 2523.
(14) Dingley, A.; Mackay, J.; Shaw, G.; Hambly, B.; King, G. *J. Biomol. NMR* **1997**, *10*, 1.
(15) Ferrage, F.; Zoonens, M.; Warschawski, D.; Popot, J.-L.; Bodenhausen, G. *J. Am. Chem. Soc.* **2003**, *125*, 2541.
(16) Sarkar, R.; Moskau, D.; Ferrage, F.; Vasos, P.; Bodenhausen, G. *J. Magn. Reson.* **2008**, *193*, 110.
(17) Riek, R.; Wider, G.; Pervushin, K.; Wüthrich, K. *Proc. Natl. Acad. Sci. U.S.A.* **1999**, *96*, 4918.
(18) Shimamura, T.; Koike-Takeshita, A.; Yokoyama, K.; Masui, R.; Murai, N.; Yoshida, M.; Taguchi, H.; Iwata, S. *Structure* **2004**, *12*, 1471.
(19) Pervushin, K.; Riek, R.; Wider, G.; Wüthrich, K. *Proc. Natl. Acad. Sci. U.S.A.* **1997**, *94*, 12366.
(20) Brutscher, B. *Concepts Magn. Reson.* **2000**, *12A*, 207.
(21) Luginbühl, P.; Wüthrich, K. *Prog. Nucl. Magn. Reson. Spectrosc.* **2002**, *40*, 199.
(22) Lee, D.; Hilty, C.; Wider, G.; Wüthrich, K. *J. Magn. Reson.* **2006**, *178*, 72.
(23) Wüthrich, K. *NMR of Proteins and Nucleic Acids*; Wiley: New York, 1986.
(24) Fiaux, J.; Bertelsen, E. B.; Horwich, A. L.; Wüthrich, K. *Nature* **2002**, *418*, 207.
(25) Riek, R.; Fiaux, J.; Bertelsen, E. B.; Horwich, A. L.; Wüthrich, K. *J. Am. Chem. Soc.* **2002**, *124*, 12144.
(26) Hedin, N.; Yu, T. Y.; Furo, I. *Langmuir* **2000**, *16*, 7548.
(27) Jerschow, A.; Müller, N. *J. Magn. Reson.* **1997**, *125*, 372.
(28) Squire, P. G.; Himmel, M. E. *Arch. Biochem. Biophys.* **1979**, *196*, 165.
(29) Atkins, P. W. *Physical Chemistry*; Oxford University Press; Oxford, U.K., 1995; p C27.